HHS Public Access

Author manuscript

Cell Rep. Author manuscript; available in PMC 2018 June 12.

Published in final edited form as:

Cell Rep. 2018 May 29; 23(9): 2629–2642. doi:10.1016/j.celrep.2018.04.111.

Aerobic Glycolysis Is Essential for Normal Rod Function and Controls Secondary Cone Death in Retinitis Pigmentosa

Lolita Petit[1], **Shan Ma**[1], **Joris Cipi**[1], **Shun-Yun Cheng**[1], **Marina Zieger**[2], **Nissim Hay**[3], and **Claudio Punzo**[1,4,*]

[1]Department of Ophthalmology and Gene Therapy Center, University of Massachusetts Medical School, Worcester, MA, USA

[2]Division of Pulmonary Medicine, Department of Pediatrics, University of Massachusetts Medical School, Worcester, MA, USA

[3]Department of Biochemistry and Molecular Genetics, College of Medicine, University of Illinois at Chicago, Chicago, IL, USA

SUMMARY

Aerobic glycolysis accounts for ~80%–90% of glucose used by adult photoreceptors (PRs); yet, the importance of aerobic glycolysis for PR function or survival remains unclear. Here, we further established the role of aerobic glycolysis in murine rod and cone PRs. We show that loss of hexokinase-2 (HK2), a key aerobic glycolysis enzyme, does not affect PR survival or structure but is required for normal rod function. Rods with HK2 loss increase their mitochondrial number, suggesting an adaptation to the inhibition of aerobic glycolysis. In contrast, cones adapt without increased mitochondrial number but require HK2 to adapt to metabolic stress conditions such as those encountered in retinitis pigmentosa, where the loss of rods causes a nutrient shortage in cones. The data support a model where aerobic glycolysis in PRs is not a necessity but rather a metabolic choice that maximizes PR function and adaptability to nutrient stress conditions.

In Brief

Photoreceptors are terminal differentiated neurons using aerobic glycolysis to meet their metabolic needs. Using a hexokinase-2 conditional mouse, Petit et al. show that photoreceptors do not need hexokinase-2 for survival but rather for function and adaptation to metabolic stress.

*Correspondence: claudio.punzo@umassmed.edu.
4Lead Contact

SUPPLEMENTAL INFORMATION

Supplemental Information includes Supplemental Experimental Procedures and seven figures and can be found with this article online at https://doi.org/10.1016/j.celrep.2018.04.111.

AUTHOR CONTRIBUTIONS

L.P. conceived and performed experiments, interpreted data, and wrote the manuscript. J.C., S.-Y.C., and S.M. performed experiments. M.Z. provided feedback. N.H. provided reagents. C.P. conceived and performed experiments and wrote the manuscript.

DECLARATION OF INTERESTS

The authors declare no competing interests.

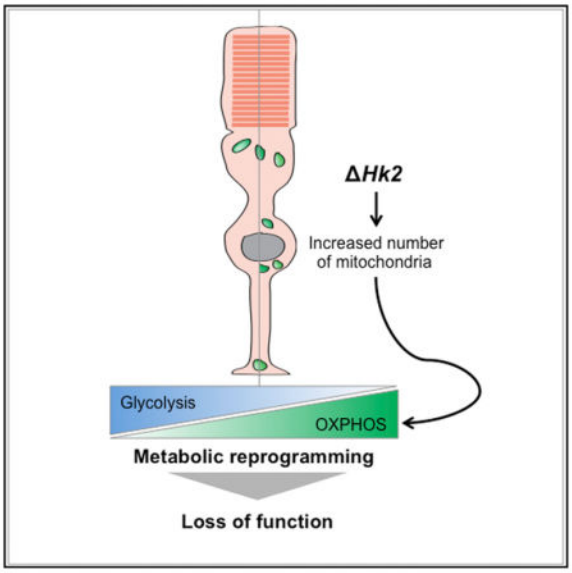

INTRODUCTION

Rod and cone photoreceptors (PRs) are the neurons ensuring light detection in the retina. Although terminally differentiated and non-proliferative, PRs are among the most metabolically active cells of the body (Ames, 2000). In the dark, they consume considerable ATP amounts to activate ion pumps in their plasma membrane that maintain membrane excitability. In the light, they use energy to support visual signal transduction (Okawa et al., 2008). While maintaining homeostasis, PRs have very high biosynthetic requirements. PRs replace daily 10% of their outer segment (OS), a protein and lipid rich organelle, that is lost to phagocytosis by the retinal pigment epithelium (RPE) (LaVail, 1976). Yet, we have to fully understand how PRs regulate metabolic pathways to meet both their energetic and anabolic demands, and how this affects PR function and survival. A better understanding of the regulation of PR metabolism is important to determine why PRs die due to energy stress in a number of human blinding diseases (Aït-Ali et al., 2015; Joyal et al., 2016; Punzo et al., 2009; Zhang et al., 2016).

Neurons depend on glucose as their main energy source (Mergenthaler et al., 2013). However, PRs particularity is to consume glucose in excess of that used for oxidative phosphorylation (OXPHOS) despite sufficient oxygen to metabolize glucose completely. Consequently, they convert most of their glucose to lactate (Chinchore et al., 2017; Cohen and Noell, 1960; Narayan et al., 2017; Wang et al., 1997; Winkler, 1981). This process, referred to as aerobic glycolysis, is a hallmark of cancer cells, where it supports unrestrained proliferation (Vander Heiden et al., 2009). In PRs, aerobic glycolysis is thought to promote the biomass necessary for OS renewal (Chinchore et al., 2017). However, the balance between aerobic glycolysis and OXPHOS in PRs *in vivo* is unknown and the importance of aerobic glycolysis for survival and function of PRs has not been evaluated. Moreover, cones and rods have different energy requirements (Hoang et al., 2002; Narayan et al., 2017;

Nikonov et al., 2008; Okawa et al., 2008; Perkins et al., 2003; Rueda et al., 2016). Whether aerobic glycolysis has the same role in both PR subtypes remains to be investigated.

Here, the importance of aerobic glycolysis in PRs was investigated by specifically inhibiting in cones and rods a gatekeeper of aerobic glycolysis: hexokinase (HK) 2 (Gershon et al., 2013; Roberts and Miyamoto, 2015; Wolf et al., 2011). HK catalyzes the first critical step of glycolysis: the ATP-dependent conversion of glucose to glucose-6-phosphate (G-6-P). Among the four mammalian HK isoenzymes, HK1 is the most ubiquitously expressed HK (Wilson, 2003). In contrast, HK2 is absent from most adult tissues (Wilson, 2003) but is overexpressed in most cancer cells as part of the general strategy to reprogram cell metabolism toward aerobic glycolysis (Gershon et al., 2013; Mathupala et al., 1997, 2006; Patra et al., 2013; Rempel et al., 1996; Roberts and Miyamoto, 2015; Wolf et al., 2011). The preferential mitochondrial localization of both HK1 and HK2 provides direct access to ATP generated by OXPHOS to promote rapid glucose phosphorylation (Arora and Pedersen, 1988; Mathupala et al., 2006). It also generates an ADP/ATP recycling mechanism to maintain high OXPHOS rates. AKT directly modulates mitochondrial HK2 (Roberts et al., 2013), which may allow tumor cells to dynamically adapt glycolysis depending on the metabolic state (Mergenthaler et al., 2012; Roberts and Miyamoto, 2015). Given that PRs express high levels of HK2 (Aït-Ali et al., 2015; Rajala et al., 2013; Reidel et al., 2011; Rueda et al., 2016), we hypothesized that HK2 couples aerobic glycolysis to PR survival and/or function. Here, we show that HK2 promotes aerobic glycolysis in PRs, and loss of HK2-mediated aerobic glycolysis correlates with increased OXPHOS. This reprogramming has no impact on PR survival rather it impairs rod function. Moreover, HK2 is required to help cones to survive under metabolic stress.

RESULTS

HK2 Is Expressed at Comparable Levels in Rods and Cones

To elucidate the role of *Hk2* and aerobic glycolysis in PRs, we first confirmed that HK2 is present in both rods and cones and that PR-specific loss of function is achieved. As expected (Aït-Ali et al., 2015; Rajala et al., 2013; Reidel et al., 2011; Rueda et al., 2016), HK2 expression was PR-enriched and increased during the postnatal maturation of PRs (Figures 1A–1C). Western blot analysis confirmed the specificity of the HK2 antibody (Figure S1A). Using the *Ai9_MCre*$^{+}$ line, which conditionally expresses the fluorescent tdTomato protein in cones, we confirmed that *Hk2* is also expressed in cones (Figures 1C and S1B). Cone expression was further validated on retinal flatmounts of *Nrl*$^{-/-}$ mice, which have no rods due to a developmental reprogramming of rods into cones (Figure S1B). Immunohistochemistry (IHC) showed that HK2 was localized to the inner segment (IS) and the synaptic terminal of PRs (Figure 1D). In cones, HK2 was also localized within the perinuclear region (Figures 1C and 1D).

Loss of HK2 function in rods or cones was achieved by crossing the *Hk2* conditional mouse (*Hk2*$^{c/c}$) to the rod-specific *iRCre* line or the cone-specific *MCre* line, respectively. Cell-type specificity and developmental expression analyses of both *Cre* lines showed that at least 89% and 100% of rods and cones, respectively, express CRE recombinase (Figures S1D and S1H), with *Cre* expression becoming evident by post-natal day (PN) 5–7 (Figures S1E and

S1F). HK2 loss was confirmed at the RNA and protein level and by IHC (Figures 1D–1G and S1I). Mice heterozygous for *Hk2* in rods ($Hk2^{c/+}$_$iRCre^{+}$) displayed a 50%–70% decrease in HK2 RNA and protein levels when compared to wild-type mice (Figures 1D–1G). To confirm the loss of HK2 in cones, we generated mice with simultaneous *Hk2* deletion in rods and cones ($Hk2^{c/c}$_$iRCre^{+}$_$MCre^{+}$*).* These mice had no residual HK2 protein in the retina (Figures 1D, 1F, and 1G). The data show that both rods and cones express HK2, and one allele is not sufficient to achieve normal expression. Additionally, the remainder of HK2 protein in $Hk2^{c/c}$_$iRCre^{+}$ mice and the complete absence of the protein after *Hk2* deletion in rods and cones suggests that cones and rods express comparable levels of HK2.

HK2 Loss Inhibits Aerobic Glycolysis in Rods

Hk2 knockout in cancer cells leads to loss of aerobic glycolysis (Wolf et al., 2011). To determine if HK2 loss also inhibits aerobic glycolysis in PRs, critical glycolysis enzymes and extracellular lactate production were evaluated in 1-month-old $Hk2^{c/c}$_ $iRCre^{-}$, $Hk2^{c/+}$_$iRCre^{+}$, and $Hk2^{c/c}$_$iRCre^{+}$ mice (Figures 2 and S2). Lactate dehydrogenase (LDH) mediates the bidirectional conversion between pyruvate and lactate and constitutes an important switch between aerobic glycolysis and OXPHOS (Valvona et al., 2016). LDH is a tetrameric enzyme composed of LDHA and LDHB subunits, which have different substrate and product affinities. Consequently, the relative proportion of LDHA and LDHB within the LDH tetramer changes the reaction rate and thereby the steady-state levels in cells. LDHA, which has a higher affinity for pyruvate, is generally associated with high rates of aerobic glycolysis (Read et al., 2001; Valvona et al., 2016). Because of that, LDHA is expressed at high levels in PRs (Casson et al., 2016; Chinchore et al., 2017; Rueda et al., 2016). We found reduced expression of LDHA after partial or total ablation of HK2 in rods (Figures 2A, 2B, and S2). In contrast, the low levels of LDHB remained unchanged (Figures 2A, 2B, and S2). Expression of pyruvate kinase muscle isozyme M2 (PKM2), another enzyme promoting anabolism (Iqbal et al., 2013, 2014), was also decreased in $Hk2^{c/c}$_$iRCre^{+}$ retinas, but no change was seen in $Hk2^{c/+}$_$iRCre^{+}$ mice (Figures 2A, 2B, and S2). Previous work established an essential role for LDHA and PKM2 in supporting lactate production by rods (LDHA and PKM2 conditional knockout decreased lactate secretion by ~57% and ~14% per Cre^{+} rods, respectively). Similarly, we observed a significant reduction in extracellular lactate in both $Hk2^{c/c}$_$iRCre^{+}$ and $Hk2^{c/+}$_$iRCre^{+}$ retinas (loss of ~39% of extracellular lactate per Cre^{+} rods, Figure 2C). Inhibiting HK2-mediated aerobic glycolysis also resulted in a significant reduction in NAPDH in $Hk2^{c/c}$_$iRCre^{+}$, but not $Hk2^{c/+}$_ $iRCre^{+}$ retinas (Figure 2C). The equivalent experiment with HK2 loss in cones was not carried out, as cones account only for 3% of PRs making it difficult to detect changes in total retinal extracts. The data indicate that at least in rods, HK2 loss inhibits aerobic glycolysis.

Minimal Cell Death in HK2-Deficient PRs

To study the effect of HK2-mediated aerobic glycolysis in PRs, we performed funduscopy and histological analyses over a 12-month period on mice with *Hk2* loss in rods (Figures 3A–3D and S3) or cones (Figures 3E–3G). Surprisingly, we found no evidence of PR cell death at any age tested in both $Hk2^{c/c}$_$iRCre^{+}$ and $Hk2^{c/c}$_$MCre^{+}$ lines. PR numbers (Figures 3B and 3F), outer nuclear layer (ONL) thickness (Figure 3C), OS length and

structure (Figures S3A–S3C) were similar to control mice. Expression of PR-specific markers was also unaffected (Figures 3D, 3G, and S3D), indicating that rods and cones survive under conditions of aerobic glycolysis deficiency.

Aerobic Glycolysis Deficiency Alters Rod, but Not Cone, Function

The long-term viability of HK2-deficient PRs allowed us to test how aerobic glycolysis supports PR function. Electroretinography (ERG) at 1 month showed an ~30% reduction in the rod scotopic a- and b-waves amplitudes in $Hk2^{c/c}$_$iRCre^{+}$ mice when compared to $Hk2^{c/c}$_$iRCre^{-}$ and $Hk2^{c/+}$_$iRCre^{+}$ mice (Figures 4A–4E and 4H). We extended these results by comparing the leading edges of the scotopic a-wave responses of $Hk2^{c/c}$_ $iRCre^{-}$, $Hk2^{c/+}$_$iRCre^{+}$, and $Hk2^{c/c}$_$iRCre^{+}$ mice after normalization (Hood and Birch, 1996-1997) (Figure 4E). The overlap of $Hk2^{c/c}$_$iRCre^{-}$ and $Hk2^{c/+}$_$iRCre^{+}$ leading edges indicates that $Hk2^{c/+}$ rods keep normal phototransduction kinetics. In $Hk2^{c/c}$_ $iRCre^{+}$ mice, the a-wave response was reduced compared to $Hk2^{c/c}$_$iRCre^{-}$ mice; yet this reduction remained constant at all times (Figure 4E), indicating that the phototransduction cascade is not slowed. The amplitude reduction likely reflects a perturbation of the dark current and/or glutamate vesicle release. Rod responses were also delayed in implicit time (Figures 4F and 4G). Interestingly, the reduction of the rod responses remained stable for up to 18 months (Figure 4H), suggesting that inhibition of aerobic glycolysis stably impairs rod function. HK2 loss in rods did not affect cone function (Figure 4I). Unlike rods, HK2 loss in cones had no effect on PR function (Figures 4J and 4K). The results further confirm metabolic differences between cones and rods and suggest that unlike rods, cones do not depend on aerobic glycolysis or that they are better able to adapt to its inhibition.

Inhibition of HK2-Mediated Aerobic Glycolysis Rebalances PR Metabolism in Rods

To understand how the inhibition of aerobic glycolysis impairs rod function, we evaluated changes in selected glycolytic pathways. PRs in culture can produce ATP via OXPHOS when aerobic glycolysis in inhibited (Chinchore et al., 2017). PR mitochondria also provide an alternative metabolic pathway for NADPH generation in isolated mouse rods under transient glucose shortage (Adler et al., 2014). We therefore assessed mitochondrial changes in HK2-deficient PRs. The mitochondrial marker voltage-dependent anion channel (VDAC) was found to be upregulated in $Hk2^{c/c}$_$iRCre^{+}$ retinas at 1 month of age when compared to control mice (Figures 5A–5C). In $Hk2^{c/+}$_$iRCre^{+}$ and control mice, VDAC staining was mainly localized to the PR IS. While a similar staining was observed in $Hk2^{c/c}$_$iRCre^{+}$ retinas, large $VDAC^{+}$ dots were also observed in the ONL with a tendency of these dots to concentrate toward the outer limiting membrane (OLM) (Figures 5A, 5C, and 5F). Similar large dots were observed with HK1 staining (Figures 5D–5F and S4A). $VDAC^{+}$ or $HK1^{+}$ large dots did not overlap with the Muller glia marker glutamine synthase (Figures 5C, 5D, and S4A) or with the cone marker cone arrestin (Figure 5E), indicating that mitochondrial changes occurred in rods. The increased VDAC expression in $Hk2^{c/c}$_$iRCre^{+}$ retinas was also associated with a marked upregulation of mitochondrial OXPHOS proteins (Figures 5G and S2B). Transmission electron microscopy confirmed a higher number of mitochondria in HK2-deficient rods compared with controls (Figures 5H, 5I, and S3E–S3G). These mitochondria were in the distal perinuclear area of the rod somas (Figures 5H, S3E, and S3F), a distribution observed in cone PRs only or in avascular retinas. The number and size

of perinuclear rod mitochondria in *Hk2*$^{c/c}$*_iRCre*$^{+}$ mice increased with age (Figures 5H and S3E).

To determine if the increase in mitochondria number associated with HK2 depletion was due to reduced glucose uptake, retinal explants were cultured in the presence of the fluorescent D-glucose analog 2-NDGB (Figures S5Aand S5B). Fluorescence intensity was decreased when 2-NBDG was inhibited by addition of D-glucose to the media. Interestingly, whereas a slight decrease was observed in *Hk2*$^{c/+}$*_iRCre*$^{+}$ retinas compared to controls, *Hk2*$^{c/c}$*_iRCre*$^{+}$ retinas showed no difference in glucose uptake when compared to controls. This maintenance in glucose uptake was associated with an upregulation of HK1 and GLUT1 at 1 and 12 months (Figures S4A, S5C, and S5D). In *Hk2*$^{c/+}$*_ iRCre*$^{+}$ retinas, no significant change in the expression of HK1 and GLUT1 were observed in total retinal extracts (Figure S5C), despite an increase in the number of HK1^{+} dots in the ONL (Figure 5F). We also observed a progressive decline in HK2 expression (Figure S4) and a compensatory upregulation of HK1 in normal rods with age (Figure S4). Thus, although glucose flux was not directly evaluated, the downregulation of enzymes critical for aerobic glycolysis along with decreased lactate levels and an increase in mitochondrial number suggest that the decrease in HK2-meditaed aerobic glycolysis is coupled to elevated OXPHOS. The absence of mitochondrial biogenesis in *Hk2*$^{c/+}$*_iRCre*$^{+}$ mice may indicate that rods engage in compensatory mechanisms to maintain a relatively high glycolytic flux that results in a decrease in lactate production with no change in PKM2, and NADPH synthesis. Therefore, increased OXPHOS largely compensates for aerobic glycolysis deficiency in rods.

In cones, only HK1, but not VDAC staining nor mitochondria number, increased upon HK2 loss, possibly reflecting the higher basal OXPHOS capacity of cones compared to rods (Perkins et al., 2003) (Figure S5E).

PRs may use lactate to fuel oxidative metabolism (Pellerin and Magistretti, 1994; Poitry-Yamate et al., 1995). Rods are the main producers of lactate in the retina (Chinchore et al., 2017; Hurley et al., 2015), thus, we considered the possibility that cones can use rod-derived lactate as an alternative fuel to compensate for glycolysis reduction. We performed ERG analyses on mice with simultaneous *Hk2* loss in rods and cones. Remarkably, cone responses were reduced in *Hk2*$^{c/c}$*_iRCre*$^{+}$*_MCre*$^{+}$ mice compared to *Hk2*$^{c/c}$*_iRCre*$^{+}$ littermates (Figure 6A), suggesting that when aerobic glycolysis is affected, cones rely on lactate produced by rods. Accordingly, we observed an increase of LDHB in cones of *Hk2*$^{c/c}$*_ iRCre*$^{+}$*_MCre*$^{+}$ mice when compared to *Hk2*$^{c/c}$*_ iRCre*$^{+}$*_MCre*$^{-}$ mice at 2 months (Figure 6B), while there was no change in LDHB expression in *Hk2*$^{c/c}$*_MCre*$^{+}$ mice compared to *Hk2*$^{c/c}$*_MCre*$^{-}$ mice at 1 (Figure 6B) or 12 months (data not shown). Thus, cones adapt to loss of *Hk2* by taking up lactate produced by rods.

Cones under Metabolic Stress Require HK2 to Survive

The balance between aerobic glycolysis and OXPHOS may be altered during disease or conditions of severe metabolic perturbations. To investigate the role of aerobic glycolysis during retinal degeneration, we crossed the *Hk2_MCre*$^{+}$ line with the *retinal degeneration 1* (*rd1*) mouse model of retinitis pigmentosa (RP). In RP, cone death always follows rod death. Accumulative evidence suggests that cones die in RP due to glucose deprivation. We showed

that cones upregulate several metabolic genes at the onset of cone death including hypoxia-induced factor 1 (HIF-1a), GLUT1, PKM2 and HK2 (Punzo et al., 2009; Venkatesh et al., 2015) suggesting that cones attempt to metabolize more glucose through aerobic glycolysis. This metabolic reprogramming in cones may be similar to the Warburg effect in cancers where tumors adapt to glucose deprivation (Amoroso et al., 2012). Consistent with this, we found that constitutive activation of the mammalian target of rapamycin complex 1 (mTORC1), through ablation of the tuberous sclerosis complex protein 1 (TSC1), confers a strong survival advantage to cones in *rd1* mice (Venkatesh et al., 2015). mTORC1 regulates aerobic glycolysis. Its constitutive activation further enhanced the expression of the aforementioned genes and of retinal NAPDH levels, likely improving the efficacy and durability of this natural protective mechanism. Moreover, subretinal injection of exogenous glucose (Wang et al., 2016) or overexpression of the rod-derived cone viability factor, which indirectly increases glucose uptake and aerobic glycolysis in cones (Aït-Ali et al., 2015), have both also been shown to improve cone survival, further attributing a central role to glucose during secondary cone death in RP.

We used the Ai9 reporter mice to score for cone survival. Contrary to the cone marker cone arrestin, Cre-mediated expression of td-Tomato in *rd1* cones does not decrease in degenerating cones (Figure S6). At 2 months, we found decreased cone survival in *rd1_Hk2*$^{c/c}$*_MCre*$^{+}$ retinas when compared to *rd1_Hk2*$^{c/+}$*_ MCre*$^{+}$ and control retinas (Figure 7). Similarly, HK2 loss abrogated the pro-survival effect of constitutively activated mTORC1 in *rd1_Tsc1*$^{c/c}$*_Hk2*$^{c/c}$*_MCre*$^{+}$ mice (Figures 7B and S7A). In the latter case, the survival effect depended on the dose of *Hk2*. These results demonstrate that improved glucose metabolism mediates cone survival upon TSC1 loss and show that HK2-mediated aerobic glycolysis allows better PR adaptability under the metabolic stress created by the loss of rods in retinitis pigmentosa. Notably, deleting HIF-1a, a key regulator of *Hk2* expression (Riddle et al., 2000) that is upregulated in cones of *rd1* mice and upon TSC1 loss in cones (Punzo et al., 2009; Venkatesh et al., 2015), had no effect on cone survival in *rd1* and *rd1_Tsc1*$^{c/c}$*_MCre*$^{+}$ mice (Figure S7). Thus, HIF-1a does not regulate HK2 in *rd1* and *rd1_Tsc1*$^{c/c}$*_MCre*$^{+}$ cones.

DISCUSSION

Since its initial observations by Otto Warburg, aerobic glycolysis has been documented in nearly all embryonic and rapidly proliferating cells, where it plays a fundamental role in supporting cell growth (Vander Heiden et al., 2009). However, why post-mitotic PRs also perform aerobic glycolysis has remained unclear. In this work, we (1) identified HK2 as a key regulator of aerobic glycolysis in PRs, and (2) revealed the importance of HK2-mediated aerobic glycolysis for PR function and survival *in vivo*. We found that HK2-mediated aerobic glycolysis is not a necessity for PR survival. Yet, aerobic glycolysis is required for optimal rod function and for the survival of nutrient-deprived cones. Based on our data, we propose that aerobic glycolysis is a metabolic choice carried out to maximize overall PR health.

PRs Can Adapt Their Metabolism

We obtained compelling evidence that PRs are able to reprogram their energy metabolism from aerobic glycolysis to increased OXPHOS upon HK2 loss. First, we found that reduction of aerobic glycolysis in HK2-deficient rods does not affect glucose uptake (Figure S5). This suggests that HK2 loss inhibits glycolysis without causing PRs to catabolize alternative energy substrates. Glucose may now be preferentially diverted toward the mitochondria. Second, we found that rods progressively increase the number of their mitochondria when HK2-mediated aerobic glycolysis is inhibited (Figures 5, S2, S3, and S4), probably to generate more ATP. Reduction of aerobic glycolysis in PRs decreases by ~20% the retinal ATP production (Ames et al., 1992; Chinchore et al., 2017; Winkler, 1981), accounting for ~50% of ATP produced by PRs (Chertov et al., 2011). Yet, PR mitochondria operate at full capacity, with limited reserve to generate more ATP. Mitochondria may thus replicate to meet the energy demands of PRs in the absence of HK2. In human neural progenitor cells (Zheng et al., 2016) and hepatocellular carcinoma (DeWaal et al., 2018), HK2 loss also marks the transition from aerobic glycolysis to OXPHOS. In isolated mouse retinas, inhibition of aerobic glycolysis did not change ATP levels, but resulted in a greater fraction of the ATP pool that is sensitive to inhibition of mitochondrial function (Chinchore et al., 2017). While our study documents PR flexibility between aerobic glycolysis and OXPHOS *in vivo*, the mechanisms linking Hk2 loss with decreased LDHA and PKM2 expression (Woo et al., 2015) and enhanced OXPHOS (DeWaal et al., 2018) require still further exploration.

Interestingly, rods show signs of similar metabolic flexibility with age. At 12 months, we found that HK2 expression was reduced while HK1 expression and mitochondria number increased (Figure S4). In line with our results, lactate production in the mouse retina decreases from 6 to 32 months (Kanow et al., 2017), whereas PR mitochondrial dynamics increases (Kam and Jeffery, 2015). Age-related thickening of the Bruch's membrane may be associated with reduced metabolic exchange that restricts the nutrient supply to PRs (Dithmar et al., 2000). Alternatively, the aging RPE may become more glycolytic, thereby reducing glucose available to PRs (Kanow et al., 2017).

Cones are less dependent on glycolysis than rods as they did not further increase their mitochondrial content upon HK2 loss (Figure S5). This is probably because cones already have a higher capacity for OXPHOS (Perkins et al., 2003), they buffer ATP more efficiently than rods (Rueda et al., 2016), and/or because they can efficiently metabolize other fuels. Accordingly, extreme changes in glucose levels (Macaluso et al., 1992) or iodoacetic acid-mediated inhibition of glycolysis affects rods more than cones (Wang et al., 2011).

Aerobic Glycolysis Is Required for Optimal Rod Function

Interestingly, the increase in the number of mitochondria after HK2 loss in rods did not substitute completely for aerobic glycolysis as seen by the reduction in rod function (Figure 4). This result is in agreement with previous *ex vivo* studies (Winkler, 1981). Aerobic glycolysis in the retina is thought to promote the daily renewal of the PR OS because genetic inhibition of LDHA or PKM2 in rods reduced rod OS length (Chinchore et al., 2017). Enhanced aerobic glycolysis in PRs may allow glucose in excess to be diverged into the

pentose phosphate pathway (PPP) for the generation of more NADPH, which is necessary for lipid synthesis and recycling of the visual chromophore. Here, HK2 loss decreased NADPH. Yet, we did not observe appreciable changes in the rod OS length over 12 months (Figures 3 and S3). Another study reported no changes in the OS length upon the conditional depletion of *Pkm2* in rods (Wubben et al., 2017). Upon HK2 loss, HK1 and OXPHOS upregulation may compensate for the reduction of glucose driven biosynthesis through the PPP, by increasing NADPH and tricarboxylic acid (TCA) cycle intermediates used as precursors for fatty acids synthesis (Adler et al., 2014). Upon LDHA loss, this compensatory mechanism may be less present and/or anabolic pathways may be more affected. Consistent with this, we observed that partial or total loss of HK2 in rods did not have the same effects on glucose uptake, glycolytic gene expression and mitochondrial biogenesis, despite a similar reduction in lactate production (Figure 2).

Our data support the hypothesis that aerobic glycolysis is a source of ATP for rod terminal processes (Rueda et al., 2016). Rod synaptic terminal express high levels of HK2, but not HK1, contain high levels of the liver isoform of phosphofructokinase (PFK-L) and high LDH activity, but low cytochrome *c* oxidase activity compared to the IS (Rueda et al., 2016). HK2-depleted rods experience changes in their dark current and/or glutamate vesicle recycling, two ATP-consuming processes (Figure 4). Moreover, HK2-depleted rods exhibit perinuclear mitochondria, which are only seen in avascular retinas where there is a problem for ATP-dependent reactions at the synaptic terminal (Linton et al., 2010; Stone et al., 2008).

Aerobic Glycolysis Contributes to Retinitis Pigmentosa Pathogenesis

Although genetic and environmental factors contribute to PR degenerative diseases, the underlying etiology common to many such diseases may be dysregulated metabolism of these metabolically demanding cells (Aït-Ali et al., 2015; Joyal et al., 2016; Punzo et al., 2009; Venkatesh et al., 2015; Zhang et al., 2016; Zieger and Punzo, 2016). Thus, understanding what PRs need to survive could lead to mutation-independent therapies that could be broadly applicable (Petit et al., 2016). We have provided evidence that HK2-mediated aerobic glycolysis helps cones to adapt to the metabolic stress created by the loss of rod in RP. Our data corroborate previous findings that glucose might be the limiting factor for cone survival during disease. Intuitively it would make more sense that cones make most of the limited glucose through OXPHOS. However, cones prefer to use the glucose available through aerobic glycolysis, maybe because besides ATP, it may also provide most of the NADPH and building blocks required for anabolism. Accordingly, the reduction in cone function in HK2 double mutant mice, suggests that cones may partially rely on other fuels to meet their high ATP needs when under stress (Figure S5). In this regard, we did not observe increased AMP-kinase phosphorylation in *rd1* cones at the onset of cone death (data not shown). The low glucose availability in *rd1* cones likely creates an NAPDH shortage that becomes detrimental. Indeed, we showed that loss of the NADPH-dependent apoptotic *Caspase-2* prolongs cones survival in *rd1* mice, while constitutive mTORC1 activation improved durability of this aerobic glycolysis-driven defense (Venkatesh et al., 2015). Further studies are needed to determine how enhanced aerobic glycolysis enhances NADPH production or consumption. In the meantime, the observation that ‘‘forced’’ aerobic glycolysis in neurons causes detrimental pyruvate depletion and ATP shortage upon limited

glucose uptake warrants further examination (Zheng et al., 2016). ‘‘Forced’’ aerobic glycolysis may be both friend and foe to PR survival, depending on the circumstance.

EXPERIMENTAL PROCEDURES

Animals

Ai9 Cre reporter, *Pde6β*$^{rd1/rd1}$ (referred as *rd1*), C57BL/6J, *Hif1a*$^{c/c}$, and *Tsc1*$^{c/c}$ mice were purchased from Jackson Laboratories. The *Nrl*$^{-/-}$ (Mears et al., 2001), the cone-*Cre* mice (referred as M*Cre*) (Le et al., 2004), the rod iCre-75 mice (referred as iR*Cre*) (Li et al., 2005), and the *Hk2*$^{c/c}$ mice (Patra et al., 2013) were kindly provided by Drs. H. Khanna, Y.Z. Le, C.K. Chen, and N. Hay, respectively. All animal procedures were approved by the university’s Institutional Animal Care and Use Committee (IACUC). Ages of animals varied between 1–12 months as indicated in figures. Male and female mice were used in equal numbers unless indicated.

Electroretinography and Funduscopy

Electroretinography (ERG) and funduscopy were carried out as previously described (Hood and Birch, 1996–1997; Ma et al., 2015; Venkatesh et al., 2013).

Quantification of Cre$^+$ Cells Using Flow Cytometry

Retinas from 2 *Ai9*$^{+/+}$_*MCre*$^+$ mice and 2 *Ai9*$^{+/+}$_iR*Cre*$^+$ mice were pooled and dissociated into single cells by papain digestion. Td-Tomato$^+$ cells were quantified using flow cytometry.

Immunohistochemistry

Immunohistochemistry (IHC) was performed on retinal cryosections (20 μm) as described previously (Venkatesh et al., 2013) with a minimum of 3 mice per line. An antibody list is presented in the Supplemental Information.

Quantification of PR Survival

Quantification of rod survival was performed on retinal cross-sections by measuring the thickness of the ONL and counting all ONL nuclei within 3–5 consecutive sections per eye (Petit et al., 2017). Quantification of cone survival was performed on retinal flat-mounts by counting all cones over the entire retinal surface. Antibody staining and tiling of retina was performed as described (Venkatesh et al., 2015). Ai9$^+$, PNA$^+$, LM opsin$^+$, or S opsin$^+$ cones and ONL nuclei were automatically counted using Imaris software.

Transmission Electron Microscopy

Electron microscopy was carried out as previously described (Ma et al., 2015) with 3 mice per line. OS length was measured at multiple locations on semi-thin sections. Mitochondria number per ONL cell was determined on randomly acquired TEM images by counting >200 PR cells per mouse.

Quantitative Western Blots

HK2 expression analysis during development used 4-pooled retinas from 3 mice per time point. The metabolic gene expression analysis used 2-pooled retinas from 1 mouse as one biological sample. Five to 8 biological samples were analyzed per line. Protein extracts from liver of adult C57/Bl6 mice and HEK293 cells were used as negative and positive controls, respectively. Protein extracts were prepared as described (Petit et al., 2012). Detailed procedures and antibodies are presented in the Supplemental Information.

Real-Time qPCR

Retinas from one mouse were pooled to isolate total RNA using TRIzol (Invitro Life Technologies). Total RNA was treated with DNase I, reverse-transcribed using random hexamer primers, and real-time qPCR was performed using a Bio-Rad CFX96. Two to 3 biological samples were analyzed per line. Primers and protocols are presented in the Supplemental Information.

Glucose Uptake Assay

Retinas were dissected in cold DMEM, cultured for 45 min at 37°C in DMEM medium with or without D-glucose in the presence of the fluorescent glucose analog 2-deoxy-D-glucose (2-NBDG, 1 μM), washed 4 times with ice-cold PBS and DAPI, flat-mounted between 2 pre-chilled cover slides, and imaged immediately (<10 min). Images were taken at the level of the PR segments at 5 different locations. Measurements represent duplicates of 2 experiments each.

Lactate and NADPH Assay

Lactate (Lactate assay kit: Eton Bioscience) and NADPH (Fluoro NADP/NADPH: Cell Technology) assays were performed in triplicate using 2–3 biological samples, with each biological sample consisting of 2 retinas. Retinas were dissected in ice cold DMEM, rinsed in PBS, sonicated in assay buffer, and processed following manufacturer's instructions. Results were normalized per retina.

Statistical Analysis

The Student's t test was used with following significance levels: *$p < 0.05$; **$p < 0.01$; ***$p < 0.0001$. Bar graphs indicate mean and SD. Required sample sizes were determined using G*Power 3.1 based on the effect sizes obtained with two Cre^+ and two Cre^- biological samples (each containing 2 retinas from 1 animal). Test conditions: $\alpha = 0.05$, power = 0.9. Biological samples used for sample size calculation were added to the final n numbers. Achieved power was >0.92 for all tests, except for expression changes of GLUT1 (0.535) and Complex II (0.879).

Supplementary Material

Refer to Web version on PubMed Central for supplementary material.

Acknowledgments

We are grateful to Hemant Khanna, Yun Z. Le, and Ching-Kang Chen for providing reagents. This work was supported by a grant from the ‘‘Information Recherche Retinite Pigmentaire’’ Association (to L.P.) and by the US NIH (R01-EY023570 to C.P. and R01-CA206167 to N.H.). L.P. acknowledges the Fulbright/Fondation Monahan Postdoctoral Fellowship, the Fondation de France ‘‘Young researcher in ophthalmology’’ Fellowship, and the Association Francaise contre les Myopathies Postdoctoral Fellowship. N.H. acknowledges the VA Merit Award BX000733.

References

Adler L 4th, Chen C, Koutalos Y. Mitochondria contribute to NADPH generation in mouse rod photoreceptors. J Biol Chem. 2014; 289:1519–1528. [PubMed: 24297174]

Aït-Ali N, Fridlich R, Millet-Puel G, Clérin E, Delalande F, Jaillard C, Blond F, Perrocheau L, Reichman S, Byrne LC, et al. Rod-derived cone viability factor promotes cone survival by stimulating aerobic glycolysis. Cell. 2015; 161:817–832. [PubMed: 25957687]

Ames A 3rd. CNS energy metabolism as related to function. Brain Res Brain Res Rev. 2000; 34:42–68. [PubMed: 11086186]

Ames A 3rd, Li YY, Heher EC, Kimble CR. Energy metabolism of rabbit retina as related to function: high cost of Na+ transport. J Neurosci. 1992; 12:840–853. [PubMed: 1312136]

Amoroso F, Falzoni S, Adinolfi E, Ferrari D, Di Virgilio F. The P2X7 receptor is a key modulator of aerobic glycolysis. Cell Death Dis. 2012; 3:e370. [PubMed: 22898868]

Arora KK, Pedersen PL. Functional significance of mitochondrial bound hexokinase in tumor cell metabolism. Evidence for preferential phosphorylation of glucose by intramitochondrially generated ATP. J Biol Chem. 1988; 263:17422–17428. [PubMed: 3182854]

Casson RJ, Wood JP, Han G, Kittipassorn T, Peet DJ, Chidlow G. M-type pyruvate kinase isoforms and lactate dehydrogenase A in the mammalian retina: metabolic implications. Invest Ophthalmol Vis Sci. 2016; 57:66–80. [PubMed: 26780311]

Chertov AO, Holzhausen L, Kuok IT, Couron D, Parker E, Linton JD, Sadilek M, Sweet IR, Hurley JB. Roles of glucose in photoreceptor survival. J Biol Chem. 2011; 286:34700–34711. [PubMed: 21840997]

Chinchore Y, Begaj T, Wu D, Drokhlyansky E, Cepko CL. Glycolytic reliance promotes anabolism in photoreceptors. eLife. 2017; 6:e25946. [PubMed: 28598329]

Cohen LH, Noell WK. Glucose catabolism of rabbit retina before and after development of visual function. J Neurochem. 1960; 5:253–276. [PubMed: 13810977]

DeWaal D, Nogueira V, Terry AR, Patra KC, Jeon SM, Guzman G, Au J, Long CP, Antoniewicz MR, Hay N. Hexokinase-2 depletion inhibits glycolysis and induces oxidative phosphorylation in hepatocellular carcinoma and sensitizes to metformin. Nat Commun. 2018; 9:446. [PubMed: 29386513]

Dithmar S, Curcio CA, Le NA, Brown S, Grossniklaus HE. Ultrastructural changes in Bruch’s membrane of apolipoprotein E-deficient mice. Invest Ophthalmol Vis Sci. 2000; 41:2035–2042. [PubMed: 10892840]

Gershon TR, Crowther AJ, Tikunov A, Garcia I, Annis R, Yuan H, Miller CR, Macdonald J, Olson J, Deshmukh M. Hexokinase-2-mediated aerobic glycolysis is integral to cerebellar neurogenesis and pathogenesis of medulloblastoma. Cancer Metab. 2013; 1:2. [PubMed: 24280485]

Hoang QV, Linsenmeier RA, Chung CK, Curcio CA. Photo-receptor inner segments in monkey and human retina: mitochondrial density, optics, and regional variation. Vis Neurosci. 2002; 19:395–407. [PubMed: 12511073]

Hood DC, Birch DG. Assessing abnormal rod photoreceptor activity with the a-wave of the electroretinogram: applications and methods. Doc Ophthalmol. 1996–1997; 92:253–267.

Hurley JB, Lindsay KJ, Du J. Glucose, lactate, and shuttling of metabolites in vertebrate retinas. J Neurosci Res. 2015; 93:1079–1092. [PubMed: 25801286]

Iqbal MA, Siddiqui FA, Gupta V, Chattopadhyay S, Gopinath P, Kumar B, Manvati S, Chaman N, Bamezai RN. Insulin enhances metabolic capacities of cancer cells by dual regulation of glycolytic enzyme pyruvate kinase M2. Mol Cancer. 2013; 12:72. [PubMed: 23837608]

Iqbal MA, Gupta V, Gopinath P, Mazurek S, Bamezai RN. Pyruvate kinase M2 and cancer: an updated assessment. FEBS Lett. 2014; 588:2685–2692. [PubMed: 24747424]

Joyal JS, Sun Y, Gantner ML, Shao Z, Evans LP, Saba N, Fredrick T, Burnim S, Kim JS, Patel G, et al. Retinal lipid and glucose metabolism dictates angiogenesis through the lipid sensor Ffar1. Nat Med. 2016; 22:439–445. [PubMed: 26974308]

Kam JH, Jeffery G. To unite or divide: mitochondrial dynamics in the murine outer retina that preceded age related photoreceptor loss. Oncotarget. 2015; 6:26690–26701. [PubMed: 26393878]

Kanow MA, Giarmarco MM, Jankowski CS, Tsantilas K, Engel AL, Du J, Linton JD, Farnsworth CC, Sloat SR, Rountree A, et al. Biochemical adaptations of the retina and retinal pigment epithelium support a metabolic ecosystem in the vertebrate eye. eLife. 2017; 6:e28899. [PubMed: 28901286]

LaVail MM. Rod outer segment disk shedding in rat retina: relationship to cyclic lighting. Science. 1976; 194:1071–1074. [PubMed: 982063]

Le YZ, Ash JD, Al-Ubaidi MR, Chen Y, Ma JX, Anderson RE. Targeted expression of Cre recombinase to cone photoreceptors in transgenic mice. Mol Vis. 2004; 10:1011–1018. [PubMed: 15635292]

Li S, Chen D, Sauvé Y, McCandless J, Chen YJ, Chen CK. Rhodopsin-iCre transgenic mouse line for Cre-mediated rod-specific gene targeting. Genesis. 2005; 41:73–80. [PubMed: 15682388]

Linton JD, Holzhausen LC, Babai N, Song H, Miyagishima KJ, Stearns GW, Lindsay K, Wei J, Chertov AO, Peters TA, et al. Flow of energy in the outer retina in darkness and in light. Proc Natl Acad Sci USA. 2010; 107:8599–8604. [PubMed: 20445106]

Ma S, Venkatesh A, Langellotto F, Le YZ, Hall MN, Rüegg MA, Punzo C. Loss of mTOR signaling affects cone function, cone structure and expression of cone specific proteins without affecting cone survival. Exp Eye Res. 2015; 135:1–13. [PubMed: 25887293]

Macaluso C, Onoe S, Niemeyer G. Changes in glucose level affect rod function more than cone function in the isolated, perfused cat eye. Invest Ophthalmol Vis Sci. 1992; 33:2798–2808. [PubMed: 1526729]

Mathupala SP, Rempel A, Pedersen PL. Aberrant glycolytic metabolism of cancer cells: a remarkable coordination of genetic, transcriptional, post-translational, and mutational events that lead to a critical role for type II hexokinase. J Bioenerg Biomembr. 1997; 29:339–343. [PubMed: 9387094]

Mathupala SP, Ko YH, Pedersen PL. Hexokinase II: cancer's double-edged sword acting as both facilitator and gatekeeper of malignancy when bound to mitochondria. Oncogene. 2006; 25:4777–4786. [PubMed: 16892090]

Mears AJ, Kondo M, Swain PK, Takada Y, Bush RA, Saunders TL, Sieving PA, Swaroop A. Nrl is required for rod photoreceptor development. Nat Genet. 2001; 29:447–452. [PubMed: 11694879]

Mergenthaler P, Kahl A, Kamitz A, van Laak V, Stohlmann K, Thomsen S, Klawitter H, Przesdzing I, Neeb L, Freyer D, et al. Mitochondrial hexokinase II (HKII) and phosphoprotein enriched in astrocytes (PEA15) form a molecular switch governing cellular fate depending on the metabolic state. Proc Natl Acad Sci USA. 2012; 109:1518–1523. [PubMed: 22233811]

Mergenthaler P, Lindauer U, Dienel GA, Meisel A. Sugar for the brain: the role of glucose in physiological and pathological brain function. Trends Neurosci. 2013; 36:587–597. [PubMed: 23968694]

Narayan DS, Chidlow G, Wood JP, Casson RJ. Glucose metabolism in mammalian photoreceptor inner and outer segments. Clin Experiment Ophthalmol. 2017; 45:730–741. [PubMed: 28334493]

Nikonov SS, Brown BM, Davis JA, Zuniga FI, Bragin A, Pugh EN Jr, Craft CM. Mouse cones require an arrestin for normal inactivation of phototransduction. Neuron. 2008; 59:462–474. [PubMed: 18701071]

Okawa H, Sampath AP, Laughlin SB, Fain GL. ATP consumption by mammalian rod photoreceptors in darkness and in light. Curr Biol. 2008; 18:1917–1921. [PubMed: 19084410]

Patra KC, Wang Q, Bhaskar PT, Miller L, Wang Z, Wheaton W, Chandel N, Laakso M, Muller WJ, Allen EL, et al. Hexokinase 2 is required for tumor initiation and maintenance and its systemic deletion is therapeutic in mouse models of cancer. Cancer Cell. 2013; 24:213–228. [PubMed: 23911236]

Pellerin L, Magistretti PJ. Glutamate uptake into astrocytes stimulates aerobic glycolysis: a mechanism coupling neuronal activity to glucose utilization. Proc Natl Acad Sci USA. 1994; 91:10625–10629. [PubMed: 7938003]

Perkins GA, Ellisman MH, Fox DA. Three-dimensional analysis of mouse rod and cone mitochondrial cristae architecture: bioenergetic and functional implications. Mol Vis. 2003; 9:60–73. [PubMed: 12632036]

Petit L, Lhériteau E, Weber M, Le Meur G, Deschamps JY, Provost N, Mendes-Madeira A, Libeau L, Guihal C, Colle MA, et al. Restoration of vision in the pde6β-deficient dog, a large animal model of rod-cone dystrophy. Mol Ther. 2012; 20:2019–2030. [PubMed: 22828504]

Petit L, Khanna H, Punzo C. Advances in gene therapy for diseases of the eye. Hum Gene Ther. 2016; 27:563–579. [PubMed: 27178388]

Petit L, Ma S, Cheng SY, Gao G, Punzo C. Rod outer segment development influences AAV-mediated photoreceptor transduction after subretinal injection. Hum Gene Ther. 2017; 28:464–481. [PubMed: 28510482]

Poitry-Yamate CL, Poitry S, Tsacopoulos M. Lactate released by Müller glial cells is metabolized by photoreceptors from mammalian retina. J Neurosci. 1995; 15:5179–5191. [PubMed: 7623144]

Punzo C, Kornacker K, Cepko CL. Stimulation of the insulin/mTOR pathway delays cone death in a mouse model of retinitis pigmentosa. Nat Neurosci. 2009; 12:44–52. [PubMed: 19060896]

Rajala A, Gupta VK, Anderson RE, Rajala RV. Light activation of the insulin receptor regulates mitochondrial hexokinase. A possible mechanism of retinal neuroprotection. Mitochondrion. 2013; 13:566–576. [PubMed: 23993956]

Read JA, Winter VJ, Eszes CM, Sessions RB, Brady RL. Structural basis for altered activity of M- and H-isozyme forms of human lactate dehydrogenase. Proteins. 2001; 43:175–185. [PubMed: 11276087]

Reidel B, Thompson JW, Farsiu S, Moseley MA, Skiba NP, Arshavsky VY. Proteomic profiling of a layered tissue reveals unique glycolytic specializations of photoreceptor cells. Mol Cell Proteomics. 2011; 10:M110 002469.

Rempel A, Mathupala SP, Griffin CA, Hawkins AL, Pedersen PL. Glucose catabolism in cancer cells: amplification of the gene encoding type II hexokinase. Cancer Res. 1996; 56:2468–2471. [PubMed: 8653677]

Riddle SR, Ahmad A, Ahmad S, Deeb SS, Malkki M, Schneider BK, Allen CB, White CW. Hypoxia induces hexokinase II gene expression in human lung cell line A549. Am J Physiol Lung Cell Mol Physiol. 2000; 278:L407–L416. [PubMed: 10666126]

Roberts DJ, Miyamoto S. Hexokinase II integrates energy metabolism and cellular protection: Akting on mitochondria and TORCing to autophagy. Cell Death Differ. 2015; 22:248–257. [PubMed: 25323588]

Roberts DJ, Tan-Sah VP, Smith JM, Miyamoto S. Akt phosphorylates HK-II at Thr-473 and increases mitochondrial HK-II association to protect cardiomyocytes. J Biol Chem. 2013; 288:23798–23806. [PubMed: 23836898]

Rueda EM, Johnson JE Jr, Giddabasappa A, Swaroop A, Brooks MJ, Sigel I, Chaney SY, Fox DA. The cellular and compartmental profile of mouse retinal glycolysis, tricarboxylic acid cycle, oxidative phosphorylation, and ~P transferring kinases. Mol Vis. 2016; 22:847–885. [PubMed: 27499608]

Stone J, van Driel D, Valter K, Rees S, Provis J. The locations of mitochondria in mammalian photoreceptors: relation to retinal vasculature. Brain Res. 2008; 1189:58–69. [PubMed: 18048005]

Valvona CJ, Fillmore HL, Nunn PB, Pilkington GJ. The Regulation and Function of Lactate Dehydrogenase A: Therapeutic Potential in Brain Tumor. Brain Pathol. 2016; 26:3–17. [PubMed: 26269128]

Vander Heiden MG, Cantley LC, Thompson CB. Understanding the Warburg effect: the metabolic requirements of cell proliferation. Science. 2009; 324:1029–1033. [PubMed: 19460998]

Venkatesh A, Ma S, Langellotto F, Gao G, Punzo C. Retinal gene delivery by rAAV and DNA electroporation. Curr Protoc Microbiol. 2013; Chapter 14(Unit 14D.14)

Venkatesh A, Ma S, Le YZ, Hall MN, Rüegg MA, Punzo C. Activated mTORC1 promotes long-term cone survival in retinitis pigmentosa mice. J Clin Invest. 2015; 125:1446–1458. [PubMed: 25798619]

Wang L, Kondo M, Bill A. Glucose metabolism in cat outer retina. Effects of light and hyperoxia. Invest Ophthalmol Vis Sci. 1997; 38:48–55. [PubMed: 9008629]

Wang W, Fernandez de Castro J, Vukmanic E, Zhou L, Emery D, Demarco PJ, Kaplan HJ, Dean DC. Selective rod degeneration and partial cone inactivation characterize an iodoacetic acid model of Swine retinal degeneration. Invest Ophthalmol Vis Sci. 2011; 52:7917–7923. [PubMed: 21896868]

Wang W, Lee SJ, Scott PA, Lu X, Emery D, Liu Y, Ezashi T, Roberts MR, Ross JW, Kaplan HJ, Dean DC. Two-step reactivation of dormant cones in retinitis pigmentosa. Cell Rep. 2016; 15:372–385. [PubMed: 27050517]

Wilson JE. Isozymes of mammalian hexokinase: structure, subcellular localization and metabolic function. J Exp Biol. 2003; 206:2049–2057. [PubMed: 12756287]

Winkler BS. Glycolytic and oxidative metabolism in relation to retinal function. J Gen Physiol. 1981; 77:667–692. [PubMed: 6267165]

Wolf A, Agnihotri S, Micallef J, Mukherjee J, Sabha N, Cairns R, Hawkins C, Guha A. Hexokinase 2 is a key mediator of aerobic glycolysis and promotes tumor growth in human glioblastoma multiforme. J Exp Med. 2011; 208:313–326. [PubMed: 21242296]

Woo YM, Shin Y, Lee EJ, Lee S, Jeong SH, Kong HK, Park EY, Kim HK, Han J, Chang M, Park JH. Inhibition of aerobic glycolysis represses Akt/mTOR/HIF-1α axis and restores tamoxifen sensitivity in antiestrogen-resistant breast cancer cells. PLoS ONE. 2015; 10:e0132285. [PubMed: 26158266]

Wubben TJ, Pawar M, Smith A, Toolan K, Hager H, Besirli CG. Photoreceptor metabolic reprogramming provides survival advantage in acute stress while causing chronic degeneration. Sci Rep. 2017; 7:17863. [PubMed: 29259242]

Zhang L, Du J, Justus S, Hsu CW, Bonet-Ponce L, Wu WH, Tsai YT, Wu WP, Jia Y, Duong JK, et al. Reprogramming metabolism by targeting sirtuin 6 attenuates retinal degeneration. J Clin Invest. 2016; 126:4659–4673. [PubMed: 27841758]

Zheng X, Boyer L, Jin M, Mertens J, Kim Y, Ma L, Ma L, Hamm M, Gage FH, Hunter T. Metabolic reprogramming during neuronal differentiation from aerobic glycolysis to neuronal oxidative phosphorylation. eLife. 2016; 5:e13374. [PubMed: 27282387]

Zieger M, Punzo C. Improved cell metabolism prolongs photoreceptor survival upon retinal-pigmented epithelium loss in the sodium iodate induced model of geographic atrophy. Oncotarget. 2016; 7:9620–9633. [PubMed: 26883199]

Highlights

- Loss of HK2 in rod PRs inhibits aerobic glycolysis
- Inhibition of aerobic glycolysis impairs only rod function, not rod survival
- Increased OXPHOS largely compensates the inhibition of aerobic glycolysis
- HK2 confers a survival advantage in cones under metabolic stress conditions

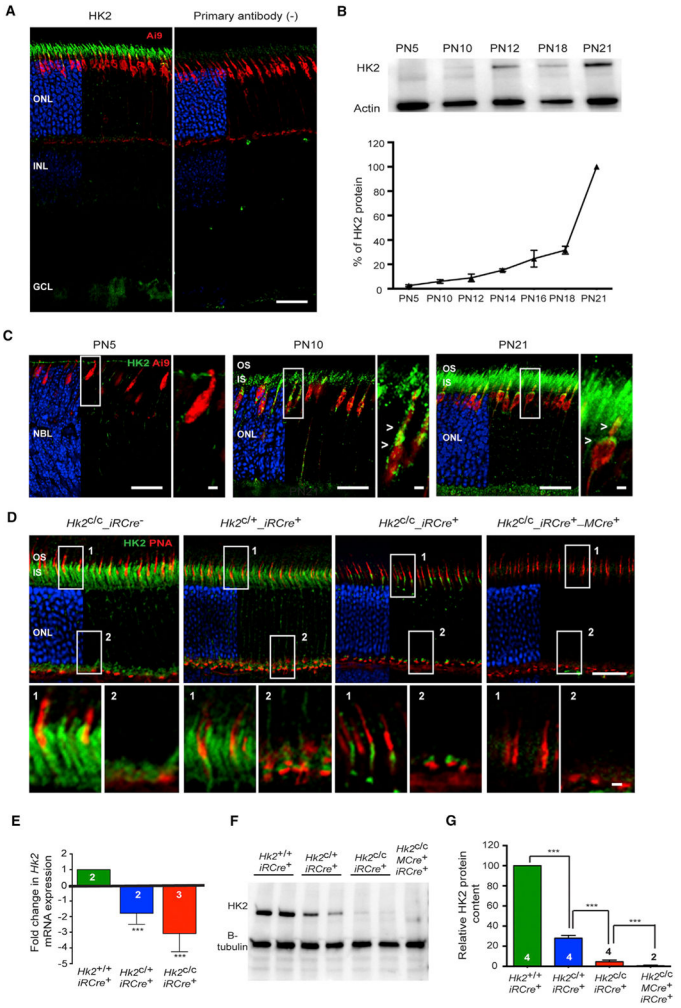

Figure 1. HK2 Expression in Cones and Rods

(A) HK2 expression (green) by IHC in adult *Ai9_MCre*$^{+}$ retinas (red: tdTomato in *Ai9_MCre*$^{+}$ mice). Right: no primary antibody. Blue: DAPI, removed from 60% of panels to visualize red and green signals.

(B) Developmental expression and quantification of HK2 by western blot with retinal extracts (loading control: actin; n = 3; levels expressed as % of PN21 levels).

(C) Developmental expression of HK2 by IHC at ages indicated with same labeling as in (A). Higher magnification of boxed area is shown to the right of each panel (arrowheads: HK2 in cones).

(D) HK2 expression (green) in retinas of genotypes indicated (red, PNA detecting cones; blue, DAPI, removed from 60% of panels to visualize red and green signals; age: 1 month). Higher magnifications of areas 1 and 2 are shown below each panel.

(E) Relative levels of retinal *Hk2* RNA after conditional *Hk2* deletion in rods (GAPDH: reference; age: 1 month).

(F and G) Western blot (F) and quantification (G) of retinal HK2 protein levels in genotypes indicated (levels expressed as % of wild-type; age: 1 month).

Errors bars ± SD; numbers in bars, number of retinas analyzed; OS, outer segment; IS, inner segment; ONL, outer nuclear layer; INL, inner nuclear layer; GCL, ganglion cell layer. Scale bars, 25 μm (long one), 5 μm (short one).

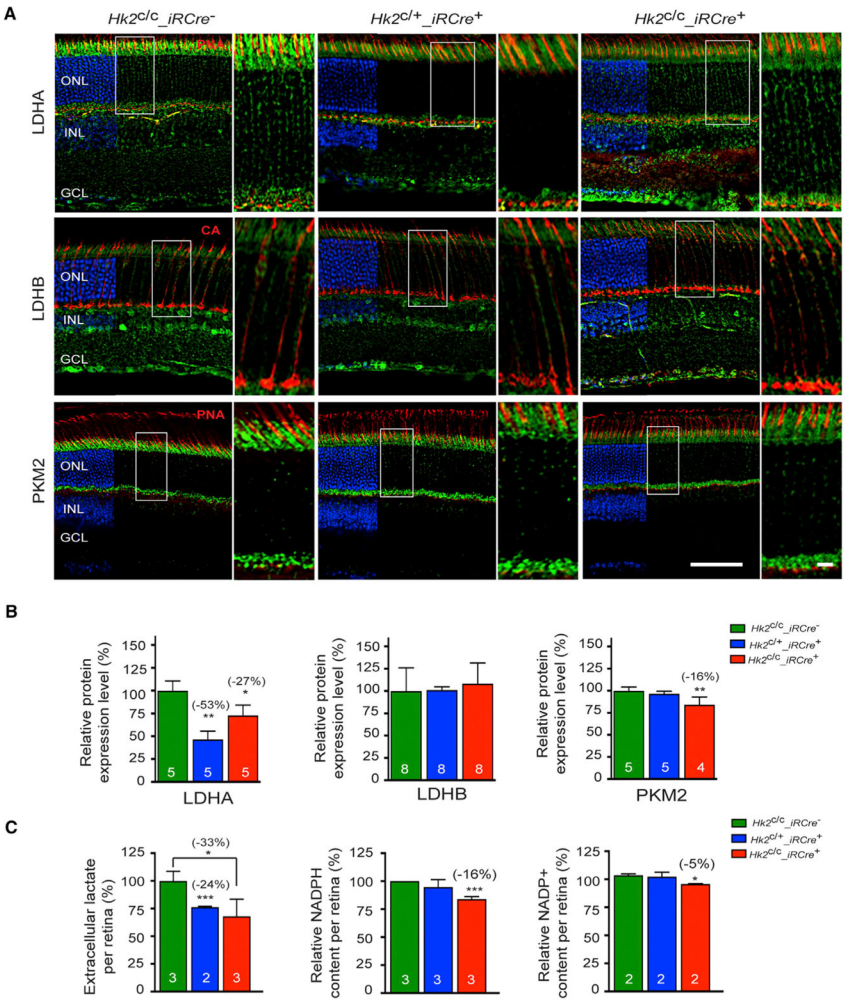

Figure 2. Changes in Aerobic Glycolysis upon HK2 Loss in Rods

(A–C) One-month-old mice of genotypes indicated in panels.

(A) IHC on retinal sections for proteins indicated to the left of each panel (green signal). Cones (red signal) were detected by PNA or with an anti-cone arrestin (CA) antibody (blue: DAPI, removed from 60% of panels to visualize red and green signals; higher magnification of boxed area is shown to the right of each panel).

(B) Quantitative western-blot analysis with retinal extracts for proteins indicated (levels expressed as % of wild-type).

(C) Quantification of lactate, NADPH and $NADP^+$ from freshly dissected retinas.

Errors bars ± SD; numbers in bars, number of biological samples (each consisting of 2 retinas from one mouse); ONL, outer nuclear layer; INL, inner nuclear layer; GCL, ganglion cell layer. Scale bars: 85 μm (long one), 10 μm (short one).

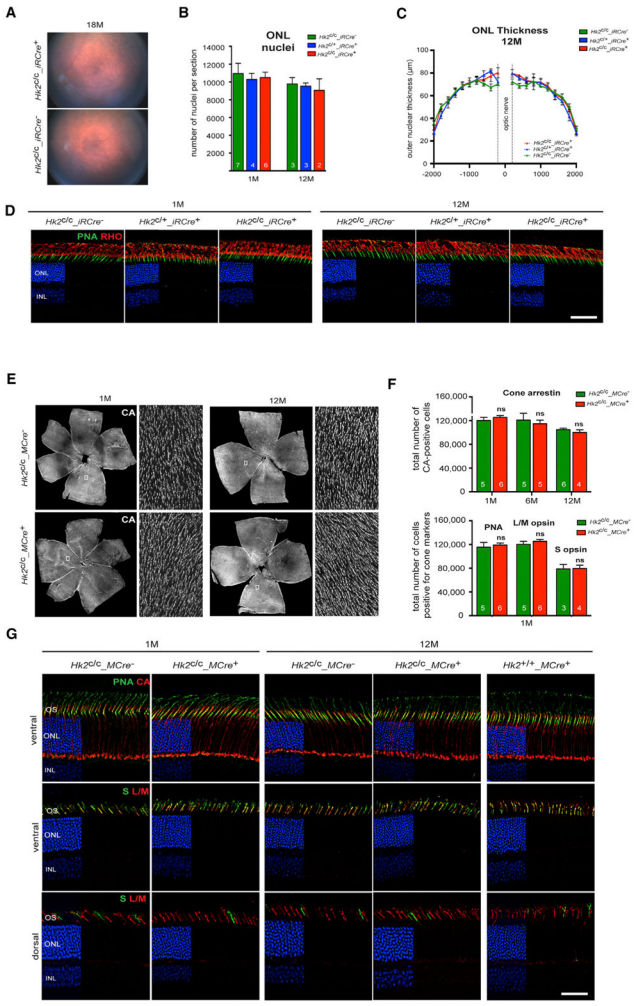

Figure 3. Rod and Cone Survival upon HK2 Loss

(A–D) Analysis of rod survival upon loss of HK2 in rods by fundus photography (A), quantification of total ONL nuclei per section (B), measurements of ONL thickness (C) and IHC on retinal sections (D) (RHO, rhodopsin red signal; PNA, green signal; blue, DAPI). (E–G) Cone survival analysis upon HK2 loss in cones performed on retinal flat mounts (E and F) stained for cone arrestin (CA) over time and PNA, medium wavelength (L/M) opsin and short wavelength (S) opsin at 1 month (F, cones per retina), and by IHC (G) for cone markers indicated in panels.

Age and genotypes as indicated: blue, DAPI (D and G), removed from 60% of panels to visualize red and green signals. Errors bars ± SD; numbers in bars, number of retinas analyzed; ONL, outer nuclear layer; INL, inner nuclear layer. Scale bars, 85 μm.

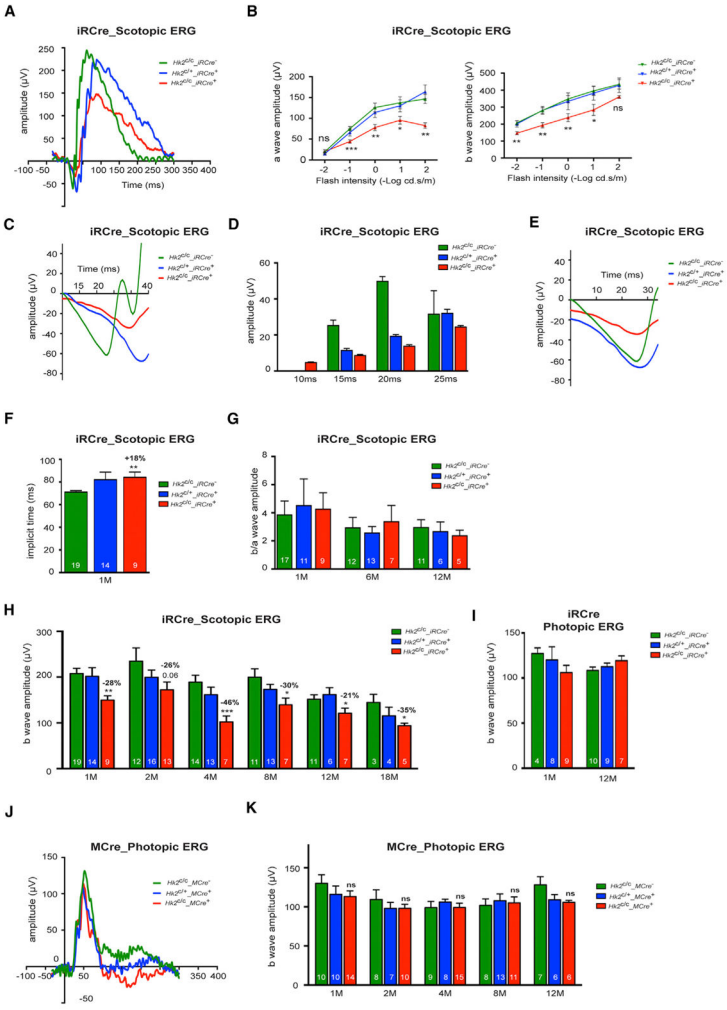

Figure 4. Analysis of Rod and Cone Function upon Loss of HK2

(A–I) Scotopic and photopic ERG recordings upon HK2 loss in rods.

(A) Representative scotopic single-flash (10 cd*s/m^2) ERG responses from 1-month-old mice.

(B) Scotopic ERG a-and b-wave responses from 1-month-old mice recorded over 5 light intensities (*Hk2$^{c/c}$_iRCre$^-$*: n = 17; *Hk2$^{c/+}$_iRCre$^+$*: n = 11; *Hk2$^{c/c}$_iRCre$^-$*: n = 9).

(C) Representative scotopic single-flash (10 cd*s/m^2) ERG responses from 1-month-old mice shown at different scales to highlight the a-wave response.

(D) Amplitude of the scotopic a-wave response at fixed time point after flash onset.

(E) Comparison of the leading edge of the scotopic a-wave (10 cd*s/m^2) after normalization (shown are representative responses as in A and C).

(F) Implicit time of b-wave responses at 1 months of age.

(G) b/a-wave amplitude ratios of scotopic ERG recorded at 0.1 cd*s/m^2 at time indicated.

(H) b-wave amplitude of scotopic single-flash ERG responses over time at 0.01 cd*s/m^2.

(I) b-wave amplitude of photopic responses at 1 and 12 months.

(J and K) Photopic ERG recordings upon loss of HK2 in cones.

(J) Representative photopic single-flash responses from 2-month-old mice.

(K) b-wave amplitude of photopic responses over time.

Errors bars ± SD; numbers in bars, number of mice analyzed.

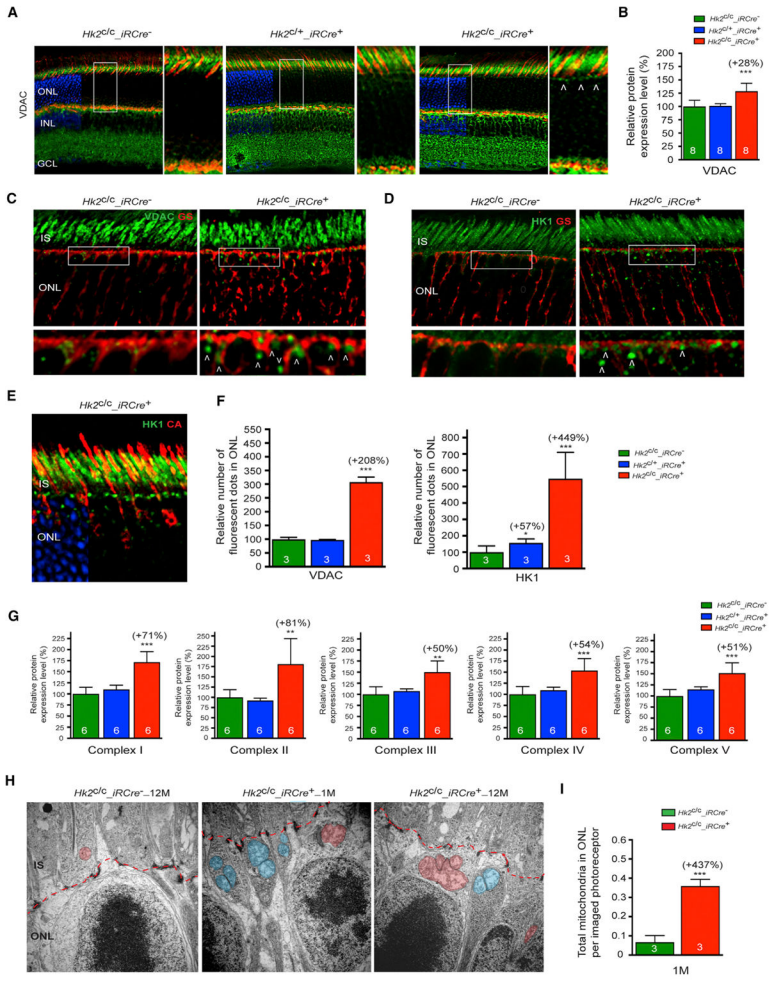

Figure 5. Increased Mitochondria Number upon Loss of HK2 in Rods

(A) Retinal sections showing increased VDAC (green, arrowheads show large VDAC^{+} dots) expression upon loss of HK2 in rods (red, PNA; blue, DAPI, removed from 60% of panels to visualize red and green signals). Boxed areas are shown to the right of each panel.

(B) Relative levels of VDAC protein assessed by western blot of total retinal extracts.

(C and D) Retinal sections stained for glutamine synthetase (GS, red) and VDAC (C, green) or HK1 (D, green) showing no colocalization of large green dots (arrowhead) with GS. Boxed areas are shown below each panel.

(E) Cross-sections of *Hk2$^{c/c}$_iRCre^{+}* retina showing that HK1 dots (green) do not co-localize with cone arrestin (CA, red; DAPI, blue, removed from 60% of panels to visualize red and green signals).

(F) Relative number of VDAC- or HK1-positive dots in the ONL.

(G) Relative level of the 5 OXPHOS complexes assessed by western blot of total retinal extracts.

(H and I) Transmission electron microscopy images (H) and mitochondria quantification (I) showing a larger number of PR mitochondria (red) in the rod perinuclear region upon loss of HK2 at 1 and 12 months (blue, mitochondria located in Mueller glia processes; red dotted line, outer limiting membrane).

Age in all experiments: 1 month except as indicated in (H); genotypes as indicated; results in (B), (F), and (G): % of wild-type. Error bars ± SD; numbers in bars, number of biological samples; ONL, outer nuclear layer; INL, inner nuclear layer; IS, inner segment; GCL, ganglion cell layer.

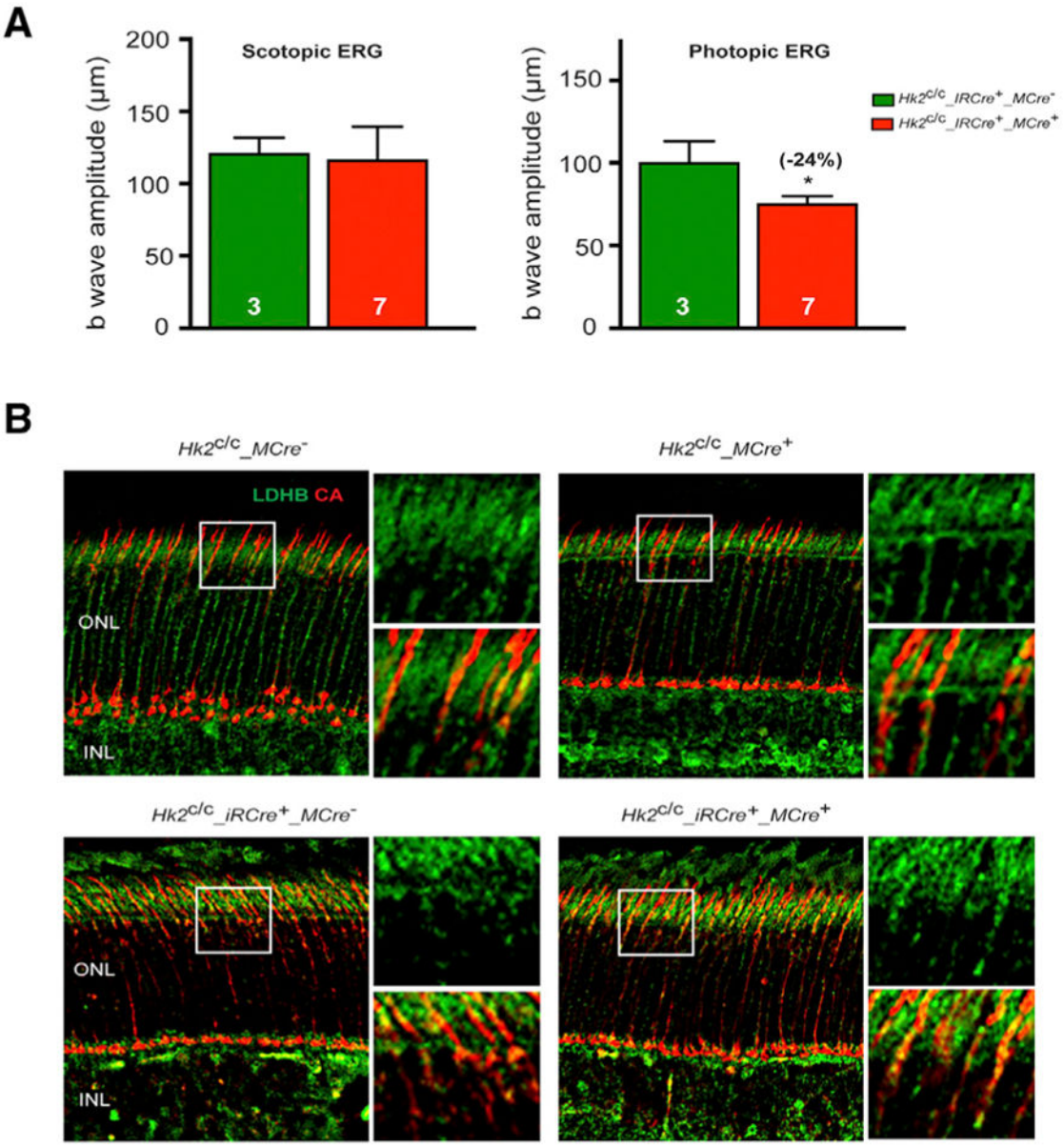

Figure 6. Retinal Function in HK2 Double Knockout Mice

(A) ERG recordings in HK2 double knockout mice at 4 months of age showing no difference in the b-wave amplitudes of scotopic single-flash ERG responses at 0.01 cd*s/m^2 between *Hk2$^{c/c}$_iRCre$^+$* and *Hk2$^{c/c}$_iRCre$^+$_MCre$^+$* littermates. In contrast b-wave amplitudes of photopic responses show reduced cone function only in *iRCre$^+$_MCre$^+$* retinas. Errors bars ± SD; numbers in bars, number of mice analyzed.

(B) Representative IHC images on retinal sections for LDHB expression (green signal) at 1 (top) or 2 (bottom) months of age. Cones were detected with an anti-cone arrestin antibody (CA, red signal). Higher magnification of boxed areas is shown to the right of each panel. INL, inner nuclear layer; ONL, outer nuclear layer.

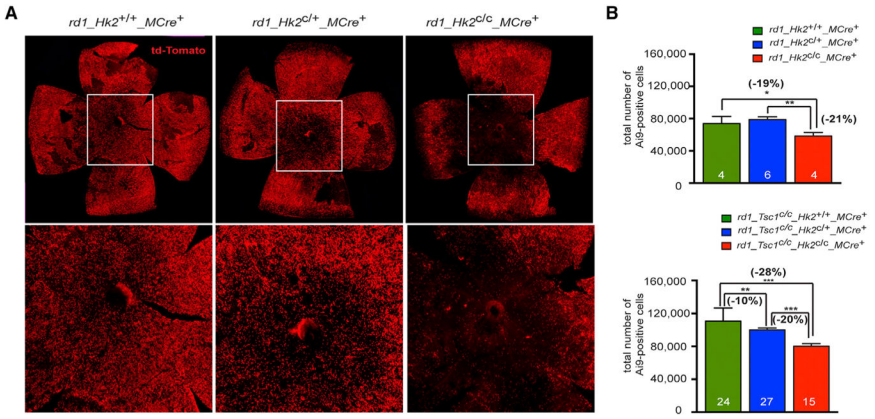

Figure 7. HK2 Promotes Cone Survival in Retinitis Pigmentosa

(A) Representative retinal flat mounts at 2 months of genotypes indicated showing less central *Ai9*$^{+}$ cones upon loss of HK2 in cones (higher magnification of boxed area).

(B) Quantification of the total number of *Ai9*$^{+}$ cones per retina at 2 months in genotypes indicated. Errors bars ± SD; numbers in bars, number of retinas analyzed.